Unfolded *in vacuo* lysozyme folds into native, quasinative, and compact structures

Gustavo A. Arteca,[1,2] I. Velázquez,[2] C. T. Reimann,[3] and O. Tapia[2,*]
[1]*Département de Chimie et Biochimie, Laurentian University, Sudbury, Ontario, Canada P3E 2C6*
[2]*Department of Physical Chemistry, Uppsala University, Box 532, S-751 21 Uppsala, Sweden*
[3]*Division of Ion Physics, Department of Material Science, Uppsala University, Box 534, S-751 21 Uppsala, Sweden*
(Received 12 January 1999)

We show that the relaxation dynamics of unfolded *in vacuo* lysozyme is not random. Analyses of molecular dynamics trajectories in a convenient space of molecular shape descriptors reveal a ''favored'' pattern of transitions leading to stable conformations. The relaxation paths exhibit a balanced change in shape features: globular spheroids are formed slowly enough to allow the proper entanglement of secondary-structural elements. The present study shows that a protein *in vacuo* can actually (re)fold into native and quasinative structures. The driving force for these transformations is intrinsic to the polypeptide chain.
[S1063-651X(99)12605-9]

PACS number(s): 87.15.Aa, 36.20.Ey

I. INTRODUCTION

Studies of protein folding and unfolding *in vacuo* and gas phase are changing the way this phenomenon is perceived both experimentally and theoretically [1–3]. In particular, mass spectrometry of biomolecular ions is providing insight into the conformations accessible to proteins in absence of solvent [1,2,4–6]. However, it remains an open question how *in vacuo* unfolded structures evolve on relaxation. Establishing whether they fold, or instead collapse in a random way, is an important issue, one whose answer may shed light on the role of solvent in biomolecular folding. This is the issue we consider in this work.

The question of how denatured proteins in solution fold into their native conformation, i.e., protein folding mechanisms, is a central problem in theoretical biophysics [7–12]. Nevertheless, the emerging picture is not yet fully satisfactory. The process is thought to be driven, to a large extent, by solvent effects. In particular, the final steps of folding, i.e., ''the endgame'' [13], are believed to be controlled by hydrophobic interactions and side-chain packing forces. However, an important piece of information is lacking: the behavior of the system in absence of solvent. Following current ideas, an unfolded protein *in vacuo* would not necessarily fold to a physiologically active conformation, since the fundamental hydrophobic driving force would be absent. In fact, before the results provided by ion-mass spectrometry of biomolecules, the very concepts of folding and unfolding of proteins *in vacuo* did not receive much attention [14]. This situation is rapidly changing [1–6].

When employing molecular dynamics (MD) to simulate the behavior of proteins far from the native conformation, one of the problems resides in the construction of a meaningful configuration space for the unfolded state [15]. The simulated unfolding of disulfide-intact lysozyme in absence of water [16] yields a sequence of transient structures compatible with a nonequilibrium refolding experiment in solution [17]. Here, we retain the hypothesis that this MD simulation produces configurations representative of the unfolded state *in vacuo* [16]. Setting up conditions to simulate folding *in vacuo* from these unfolded structures, we have carried out a number of relaxation dynamics each lasting at least 1 ns. In absence of explicit water in the simulation, any unfolded transient should somehow reorganize itself. However, if such a reorganization were to take the form of a random collapse, it would be just the opposite of a ''folding process.'' Here, we show that the relaxation of unfolded lysozyme follows instead special paths, thus suggesting the presence of a well-defined folding process *in vacuo*.

II. METHODS

In order to assess the nature of the structural rearrangements along the relaxation trajectories, we use global molecular shape descriptors that combine information on the geometry and topology of the protein backbone. Three key ingredients characterizing polymer shape are considered: the size of the chain, given by the standard radius of gyration R_g, its anisometry, measured in terms of asphericity Ω [18], and a measure of transient entanglement between loops $\overline{N}$ [18,19]. The asphericity, Ω, is given in terms of the principal moments of inertia of the α-carbon backbone $\{\lambda_i,\ i=1,2,3\}$:

$$\Omega=\frac{1}{2}\left\{\sum_{i=1}^{2}\sum_{j=i+1}^{3}(\lambda_i-\lambda_j)^2\right\}\left\{\sum_{i=1}^{3}\lambda_i\right\}^{-2}.$$

In a spheroidal globule, $\Omega=0$. In cigar-shaped molecules, $\Omega\approx\frac{1}{4}$. The degree of entanglement in a given polymer configuration is conveyed by the mean overcrossing number $\overline{N}$ defined as the number of projected crossings between backbone bonds, averaged over all projections [19]. In closed form, we have [20]

*Author to whom correspondence should be addressed. Electronic address: orlando.tapia@fki.uu.se

$$\overline{N}=\frac{1}{2\pi}\sum_{i=1}^{n-3}\sum_{j=i+2}^{n-1}\int_0^1\int_0^1\frac{|[\dot{\gamma}_i(s)\times\dot{\gamma}_j(t)]\cdot[\gamma_i(s)-\gamma_j(t)]|}{\|\gamma_i(s)-\gamma_j(t)\|^3}ds\,dt.$$

where γ_i is the segment connecting the i and $i+1$ α carbons and $\dot{\gamma}_i$ its parametric derivative along the backbone. In rodlike chains $\overline{N}\approx 0$, whereas $\overline{N}$ increases as the chain self-entangles. Helical motifs tend to produce higher overcrossing numbers than β sheets. However, $\overline{N}$ is an intrinsic global property of the backbone, and thus it is independent of how the elements of secondary structure are defined. Although a geometrical descriptor, $\overline{N}$ behaves as a weak topological invariant for DNA knots [21,22]. In the present context, $\overline{N}$ depends on the transient entanglements within the backbone of lysozyme. The descriptors $\overline{N}$ and Ω are generally uncorrelated, although large size and very elongated shapes can only be reached at the expense of reducing entanglements.

The relaxation trajectories have been determined with GROMOS87 [23]. The neutral protein model including polar hydrogens ($D4$ parameter set) was used, where hydrogen bonding is represented via electrostatic interactions [24]. For each unfolded structure, obtained from previous denaturing simulations [16], unfolding conditions are switched off, and a Maxwell-Boltzmann velocity distribution at $T=293\,\mathrm{K}$ is used. The trajectories are weakly coupled to a Berendsen thermostat [25]. With *in vacuo* boundary conditions, the whole system can freely rotate after equilibration. Temperature was constant during the trajectories. The cutoff for short-range nonbonded interactions was 0.8 nm, while it was 1.3 nm for long-range (Coulomb) interactions. No periodic boundary conditions were imposed, and SHAKE was used for bond-length constraints [26]. The integration time step used was 2 fs. Most of the trajectories were followed for 1.1 ns, while some of them were extended up to 5 ns (see below). A control run with these relaxation conditions shows a fully stable structure in a 1 ns long trajectory having most of the characteristics of the crystal structure. This will be referred to as the *in vacuo* native structure (IVNS).

All the relaxation paths exhibit essentially a one-step change in molecular *size* (as characterized by R_g) [27]. Once the initial relaxation has taken place, R_g remains virtually constant, although lysozyme still undergoes significant internal reorganizations. Moreover, most of the pathways generated settle down at similar R_g values, despite large differences in secondary structure. This lack of discrimination of R_g as a shape descriptor is known [18]. Here, we monitor instead $\overline{N}$ and Ω, which better describe the fluctuations in molecular shape [18,28].

Using the information from our relaxation MD simulations, we have established the interplay between molecular shape and accessible configurations. Below, the following questions are addressed. (a) Are there favored patterns of molecular shape changes along the relaxation paths that would allow us to properly talk of a ''folding process''? (b) Is there an interrelation between the formation of spheroidal globules and the extent to which the chain is self-entangled?

III. RESULTS

In order to contrast the shape features found during relaxation transitions, Fig. 1 shows a $(\overline{N},\Omega)$ map for representative chains with $n=129$ monomers. We include all native proteins with the same number of residues as 1 hel lysozyme, the starting point for the unfolding simulation. (Excluding redundant and obsolete entries in the Brookhaven PDB, there are 145 structures in this class, 105 of which are lysozymes.) The figure includes the approximate location of some representative tertiary folds. Also, we computed the configurationally averaged shape descriptors for off-lattice self-avoiding walks with variable excluded-volume interaction (dashed line). Values for Ω and $\overline{N}$ above the dashed line correspond to conformations with intramolecular interactions that are *not* globally attractive. Native states of globular proteins appear well below this line. Noncompact native folds (e.g., those of the viral capsids or immuglobulins) appear in regions of low entanglement, whereas nonglobular folds with high α-helical content (e.g., that of cytochrome c') appear in regions of higher entanglement and high asphericity. Finally, we note that mutations in the lysozyme sequence can produce a small (5%) variation in the mean overcrossing number of 1 hel. This noise is equivalent to an averaged crossed root-mean-square deviation (RMSD) below 0.06 nm for the set of lysozymes.

The computer-generated unfolding path [16] is indicated

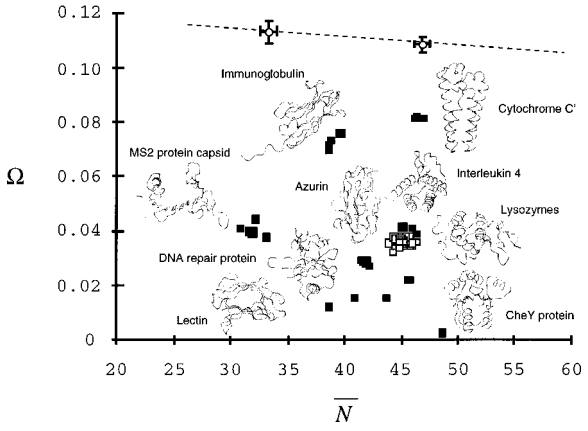

FIG. 1. Anisometry-and-entanglement map for the native folds of all available single protein chains with $n=129$ amino acid residues. Black squares represent the 40 ''nonlysozyme'' proteins, whereas the cluster of gray squares represents the lysozymes. The traced backbones indicate qualitatively the approximate location in the $(\overline{N},\Omega)$ map of the tertiary fold for a representative protein. The dashed line on the top represents the average behavior for off-lattice self-avoiding walks with variable excluded volume, 129 monomers, and a constant bond length of 0.38 nm, representative of C_α-C_α distances. The circles stand for walks with 0.15 and 0.2 nm radius of excluded volume. (Error bars are 95% confidence intervals.) The limit values for the *averaged* shape descriptors in random walks, i.e., those with no excluded volume, are $\Omega\approx 0.098$ and $\overline{N}\approx 80.4$.

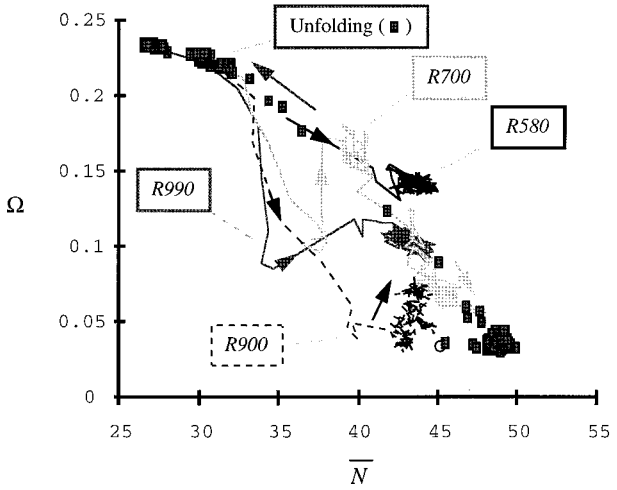

FIG. 2. Molecular shape map for the unfolding and folding pathways of 1 hel lysozyme. The unfolding path, leading from the nativelike structure to centrifugally distorted elongated proteins, is indicated by squares, corresponding to sequential snapshots separated by 5 ps. Relaxation pathways are indicated with lines. The arrows indicate the time evolution along the trajectories. The two open circles near the bottom represent the structure of native 1 hel protein in the crystal (bottom left) and the *in vacuo* native structure prior to unfolding (bottom right).

by squares in Fig. 2. We note two distinct features. (a) Before complete unfolding develops, there is a short-lived continuum of intermediate structures with similar entanglement to native lysozyme, but forming a less spherical globule. (b) The fully unfolded structures (top left corner) are very stretched configurations ($\Omega \approx 0.23$), yet exhibit a residual degree of organization in their loops, as manifested by the series of transitions in entanglement between $\overline{N} \approx 33$ and $\overline{N} \approx 25$. These structures are found above the dashed line in Fig. 1, indicating the dominance of repulsive forces.

Theoretically, two limiting behaviors connecting the extreme unfolded and the IVNS can be conceived on the $(\overline{N},\Omega)$ map: (i) relaxation paths dominated by initial collapse (decreasing Ω at constant $\overline{N}$), followed by increasing entanglement at constant Ω, (ii) paths controlled by an initial increase of $\overline{N}$, at constant Ω, up to the value representative of the native structure, followed by collapse towards the native asphericity. The latter paths would transit regions characteristic of self-avoiding walks with decreasing excluded volume (see Fig. 1). The former paths would instead visit regions representative of noncompact native folds (see Fig. 1). The relaxation trajectories in Fig. 2 show neither limiting behavior.

Let us discuss some particular examples. As seeding configurations for relaxation, we have used unfolded transients with a wide range of distortions. In all cases the unfolding was significant [16], with R_g values ranging from 1.4 nm [for $R560(0.21)$] and 1.8 nm [for $R575(0.72)$] to 3.6 nm [for $R990(1.66)$]. (The IVNS has $R_g \approx 1.3$ nm. The RMSD in nm with respect to the crystal structure is indicated in parenthesis. The code *Rxxx* for the relaxation trajectory indicates the time, as ''*xxx*'' in ps, for the unfolding intermediate used as starting structure for relaxation.) The diverse behavior in relaxation indicates that there is a manifold of accessible pathways leading to persistent (stable) intermediates. Since full unfolding begins at $t = 550$ ps, configurations that were slightly perturbed [e.g., $R560(0.21)$ or mildly perturbed $R570(0.48)$] lead back to the quasinative fold and, for the sake of clarity, are not displayed in Fig. 2. Nontrivial rearrangements are found when configurations picked up later in time are allowed to relax. Of a different kind are the $R575(0.72)$ and $R580(0.93)$ trajectories that relax following a qualitative pattern of shapes similar to those of the unfolding trajectory. However, the details of the processes are quite different. The $R575$ relaxation, also omitted for clarity, exhibits a transition in two steps leading to a structure akin (but not equal) to the IVNS. In contrast, the $R580$ (full black line) relaxation stops at a continuum of persistent structures far from the IVNS, i.e., a set of non-native structures. (For a more detailed analysis of $R575$ and $R570$, see below.)

Figure 2 shows also the relaxation of three conformations found further into the unfolding trajectory [$R700(1.35)$, $R900(1.66)$, and $R990(1.70)$]. The starting conformations are very elongated and they behave initially in a similar manner: they map the left middle region of the $(\overline{N},\Omega)$ map, above the line characteristic of off-lattice self-avoiding walks. The relaxation processes favor a rapid reduction in asphericity (i.e., compaction) leading to more spheroidal configurations. However, these transient features do *not* produce stable intermediates. In all cases, the pathways ''backtrack by inflating.'' That is, the transients *regain* asphericity and return to the swath of molecular shapes characteristic of the unfolding path. The $R900$ (dashed black) and $R990$ (gray) trajectories lead to more spheroidal transients and their relaxation into prolate structures is accompanied by an increase in entanglement. There is a moderate reduction in asphericity along the $R700$ (light gray) trajectory. In this case, the protein rapidly ''swells'' back with little change in entanglement. (These three reorganizations take place at virtually the same values of RMSD with respect to the IVNS, although the structures are different among themselves.) The analysis of the relaxation trajectories shows that lysozyme forms two sets of stable intermediates, nativelike and nonnative. Members of each class evolve while maintaining virtually constant mean size, as indicated by the RMSD and R_g values (data not shown). The changes in overcrossing number suggest an internal reorganization taking place by loop diffusion.

Figure 2 shows there is a balanced interrelation between entanglement and anisometry along the relaxation paths from highly unfolded structures. It would appear that, in order to reach persistent (stable) intermediate structures, two types of situations are *not* favored: (1) the formation of early globular conformations with little secondary structure (leading to low Ω and low $\overline{N}$ values) or (2) the formation of early conformations with high organization of secondary structure (leading to high $\overline{N}$ and intermediate Ω values).

We can regard the structures mapped during the relaxation of lysozyme in the context of the molecular shapes for native folds of proteins with $n = 129$ residues. A comparison between Figs. 1 and 2 indicates that some intermediates exhibit shapes representative of nonglobular proteins. (One must allow for a small shift in shape descriptors between the ''native'' structure *in vacuo* and that in the crystal.) For in-

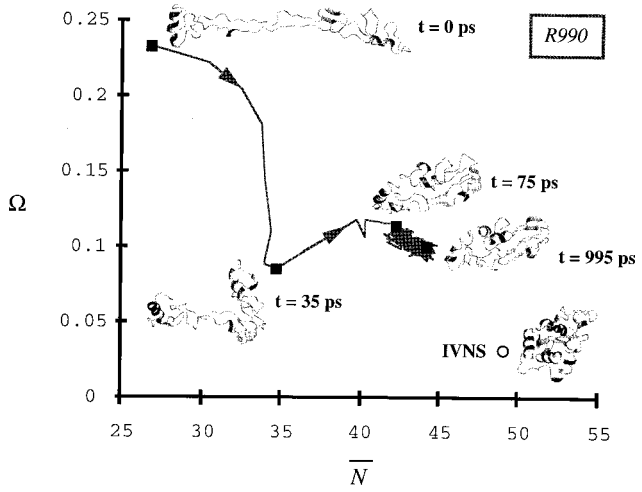

FIG. 3. Molecular shape map for representative tertiary folds found along the *R*990 relaxation trajectory. Black squares and time in picoseconds indicate the position of the snapshots. As a reference, we include a snapshot of the *in vacuo* native structure (IVNS) prior to the onset of unfolding.

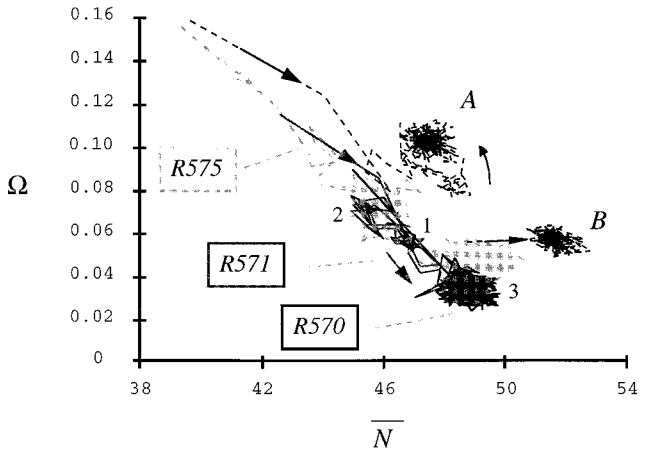

FIG. 4. Effect of pair interactions over the refolding trajectories leading to quasinative folds. The *R*570, *R*571, and *R*575 trajectories lead to quasinative conformers by using none, one, or two intermediate ''states,'' respectively. (In the case of *R*571, the final structures after 2 ns are indistinguishable from fluctuations of the native state *in vacuo*. The three ''states'' in the *R*571 trajectory are labeled 1,2,3.) The trajectories labeled *A* and *B* are recomputations of the *R*575 trajectory in which the attraction has been made more dominant (see text). In case *A*, the changes in the force field derail the prior refolding pattern.

stance, the molecular shapes at the first persistent continuum for the $R575(0.72)$ trajectory are akin to those of α-helical bundles, whereas the $R900(1.66)$ trajectory visits shapes comparable to mostly β folds (e.g., azurins and immunoglobulins). Our results suggest that relaxation pathways are biased towards stable alternative structures that are reasonable options for a protein of the same length as lysozyme. Pictorially, one can appreciate the extent of the structural reorganization from Fig. 3. For the $R990(1.66)$ trajectory, dramatic rearrangements take place without explicit presence of water. The unfolded structure reduces its asphericity while forming intermediate secondary structure elements. Thereafter, it ''inflates'' with apparent increment of secondary structure elements. The system attains a non-native folded conformation with stationary RMSD and R_g while subtle changes take place as revealed by the average overcrossing descriptor.

IV. DISCUSSION

Our main finding is that lysozyme folds *in vacuo*. The relaxation processes started from the unfolded structures signal the occurrence of nonrandom events. Instead of a simple random collapse path, our trajectories elicit what may properly be called a ''folding process.''

An enlarged $(\overline{N},\Omega)$ diagram is shown in Fig. 4 for three trajectories leading to a region near the native fold. The least perturbed trajectory [$R570(0.48)$ in full black line] contracts rapidly into a series of structures similar to (though slightly more spherical than) the native state. On the other extreme, the $R575(0.72)$ trajectory (in light gray) shows a ''two-state'' refolding transition. (These ''states'' are of course continua of interconvertible conformers sharing similar molecular shape features.) The two ''states'' in the *R*575 trajectory are qualitatively different. The first ''state,'' which is sustained for around 0.8 ns, corresponds to an ensemble of flexible structures, where asphericity and mean number of overcrossings vary over a range of values. The second ''state'' is sustained for over 4 ns, and it has a uniform oscillation in Ω over time but a slow increase in $\overline{N}$ values. This change indicates a steady ''internal diffusion'' where loops, strands, and helices accomodate relative to each other, while remaining constant both in size and anisometry.

A ''three-state'' refolding transition to the continuum of *native* structures is found in a trajectory with intermediate perturbation [$R571(0.52)$, in gray]. Moreover, this transition is achieved by following a pattern akin to the one observed in more distorted configurations. (a) After an initial contraction leading to ''state-1,'' there is an ''inflation'' transition from ''state-1'' to ''state-2.'' This transition is characterized by an increase in backbone asphericity and a decrease in entanglement complexity. (b) A transition takes place after around 300 ps, where ''state-2'' is transformed into ''state-3'' (coinciding with the IVNS) by a decrease in asphericity and a 10% increase in entanglements. As far as we know, this is the first evidence of successful refolding of a significantly-distorted protein conformation *in vacuo*, via MD simulations.

The examples in Fig. 4 underscore the subtle interplay between molecular shape and configurational fluctuations during refolding. In no case have we observed refolding as a result of a random search within shape space [29].

This delicate balance of motions must depend on the nature of the intramolecular interactions. For this reason, we have tested to what extent a change in the attractive term of the van der Waals force would affect the relaxation process. Figure 4 illustrates the effect of doing this change with two examples. The trajectories *A* and *B* (dashed black lines) correspond to MD simulations of refolding where the C_6 coefficients of the Lennard-Jones pair potential are increased by 50%. In trajectory *A*, we started the refolding from the same initial configuration used for the *R*575 trajectory. The same

procedure was used for the trajectory *B*, but in this case the simulation started from the *last* configuration reached after 5 ns along the *R*575 trajectory. Consistent with our discussion above, Fig. 4 indicates that a scaling in the van der Waals attractive interactions does not accelerate refolding but can actually change the refolding path. By making the interaction more attractive, the system appears to rigidify, thereby losing its capacity to relax the anisometry. Moreover, the conformers undergo a slight isotropic contraction leading to an increase in loop entanglement. These two results are consistent with the occurrence of configurational frustration [14]. Indeed, trajectory *A* ''recoils'' towards the dashed line in Fig. 1, suggesting that the protein is unable to reorganize further globally. We also note that, as shown by case *B*, a stronger attraction does *not* make the conformers more globular.

V. CONCLUSIONS

The global similarities among ''productive'' pathways, i.e., those yielding persistent folding intermediates, is an important finding of this work. The descriptors presented allow one to monitor all configurational transitions, including those during which molecular size or relative deviations from the IVNS remain constant. A recurrent pattern emerges: refolding to *any* stable intermediate (not necessarily native) is a compromise between forming a spheroidal globule and producing a large loop entanglement. This behavior suggests an initial ''step'' for refolding midway between the configurational collapse and the formation of secondary structures. Moreover, we have shown that there is an ensemble of ''productive'' paths, where folding to reasonable tertiary structures can start from a variety of conformers. These initial conformers were conjectured to be representative of the configurational space of the unfolded state. From these analyses, the existence of protein folding processes *in vacuo* can be inferred. The ensemble of structures along relaxation paths, epitomized by Fig. 3, may widen our understanding of current models for protein folding.

To conclude, this work shows that intramolecular forces can drive a folding process in total absence of solvent. Wolynes' conjecture [14] that proteins may fold *in vacuo* finds here a numerical support. The conditions are now ripe to reassess the details of the protein folding mechanisms and establish the specific effects of the solvent [30,31]. The knowledge of the *in vacuo* behavior may become an essential piece in solving the puzzle of protein folding [9,12,32–35].

ACKNOWLEDGMENTS

The authors thank N. D. Grant for her comments on the manuscript. G.A.A. acknowledges support from the Natural Sciences and Engineering Research Council of Canada. C.T.R. thanks the Swedish Technical Research Council (TFR) and O.T. is grateful to NFR (Swedish Natural Sciences Council) for financial support. We thank Koradi *et al.* [36] for use of the program MOLMOL.

[1] K. Shelimov and M. F. Jarrold, J. Am. Chem. Soc. **118**, 10 313 (1996).
[2] F. W. McLafferty, Z. Guan, U. Haupts, T. D. Wood, and N. L. Kelleher, J. Am. Chem. Soc. **120**, 4732 (1998).
[3] C. T. Reimann, I. Velázquez, and O. Tapia, J. Phys. Chem. B **102**, 9344 (1998).
[4] D. S. Gross, P. D. Schnier, S. E. Rodriguez-Cruz, C. K. Fagerquist, and E. K. Williams, Proc. Natl. Acad. Sci. USA **93**, 3143 (1996).
[5] J. S. Valentine, J. G. Anderson, A. D. Ellington, and D. E. Clemmer, J. Phys. Chem. B **101**, 3891 (1997).
[6] C. T. Reimann, P. A. Sullivan, J. Axelsson, A. P. Quist, S. Altman, P. Roepstorff, I. Velázquez, and O. Tapia, J. Am. Chem. Soc. **120**, 7608 (1998).
[7] A. M. Gutin, V. I. Abkevich, and E. I. Shakhnovich, Phys. Rev. Lett. **77**, 5433 (1996).
[8] C. J. Camacho, Phys. Rev. Lett. **77**, 2324 (1996).
[9] A. R. Fersht, Curr. Opin. Struct. Biol. **7**, 3 (1997).
[10] K. A. Dill and H. S. Chan, Nat. Struct. Biol. **4**, 10 (1997).
[11] S. Takada and P. G. Wolynes, Phys. Rev. E **55**, 4562 (1997).
[12] E. Shakhnovich and A. R. Fersht, Curr. Opin. Struct. Biol. **8**, 65 (1998).
[13] M. Levitt, M. Gerstein, E. Huang, S. Subbiah, and J. Tsai, Annu. Rev. Biochem. **66**, 549 (1998).
[14] P. G. Wolynes, Proc. Natl. Acad. Sci. USA **92**, 2426 (1995).
[15] W. F. van Gunsteren, P. H. Hünenberger, H. Kovacs, A. E. Mark, and C. A. Schiffer, Philos. Trans. R. Soc. London, Ser. B **348**, 49 (1995).
[16] C. T. Reimann, I. Velázquez, and O. Tapia, J. Phys. Chem. B **102**, 2277 (1998).
[17] A. Miranker, C. V. Robinson, S. E. Radford, R. T. Aplin, and C. M. Dobson, Science **262**, 896 (1993).
[18] G. A. Arteca, Macromolecules **29**, 7594 (1996).
[19] G. A. Arteca, Biopolymers **33**, 1829 (1993); Phys. Rev. E **51**, 2600 (1995).
[20] G. A. Arteca and D. I. Caughill, Can. J. Chem. **76**, 1402 (1998).
[21] V. Katritch, J. Bednar, D. Michoud, R. G. Scharein, J. Dubochet, and A. Stasiak, Nature (London) **384**, 142 (1996).
[22] A. Stasiak, V. Katritch, J. Bednar, D. Michoud, and J. Dubochet, Nature (London) **384**, 122 (1996).
[23] W. F. van Gunsteren and H. J. C. Berendsen, *Groningen Molecular Simulation (GROMOS) Library Manual* (Biomos, Groningen, 1987).
[24] J. Åqvist, W. F. van Gunsteren, M. Leijonmarck, and O. Tapia, J. Mol. Biol. **83**, 461 (1985).
[25] H. J. C. Berendsen, J. P. M. Postma, W. F. van Gunsteren, A. DiNola, and J. R. Haak, J. Chem. Phys. **81**, 3684 (1984).
[26] J.-P. Ryckaert, G. Ciccotti, and H. J. C. Berendsen, J. Comput. Phys. **23**, 327 (1977).
[27] I. Velázquez, C. T. Reimann, and O. Tapia (unpublished).
[28] G. A. Arteca, O. Nilsson, and O. Tapia, J. Mol. Graphics **11**, 193 (1993).

[29] C. J. Levinthal, in *Mössbauer Spectroscopy in Biological Systems*, edited by P. Debrunner, J. C. M. Tsibris, and E. Munck (University of Illinois Press, Urbana, 1968), p. 22; J. Chim. Phys. Phys.-Chim. Biol. **65**, 44 (1968).
[30] X. Daura, B. Jaun, D. Seebach, W. F. van Gunsteren, and A. E. Mark, J. Mol. Biol. **280**, 925 (1998).
[31] Y. Duan and P. A. Kollman, Science **282**, 740 (1998).
[32] R. L. Baldwin, Nat. Struct. Biol. **4**, 965 (1997).
[33] T. Lazaridis and M. Karplus, Science **278**, 1928 (1997).
[34] P. A. Jennings, Nat. Struct. Biol. **5**, 846 (1998).
[35] M. Gruebele and P. G. Wolynes, Nat. Struct. Biol. **5**, 662 (1998).
[36] R. Koradi, M. Billeter, and K. Wüthrich, J. Mol. Graph. **14**, 51 (1996).